What Are The Sources of Mechanical Damping in Matsuno-Gill Type Models?

Jia-Lin Lin[1], Brian E. Mapes[2], and Weiqing Han[3]

[1]NOAA ESRL/CIRES Climate Diagnostics Center, Boulder, CO
[2]RSMAS, University of Miami, Miami, FL
[3]DAOS, University of Colorado, Boulder, CO

Submitted to *J. Climate*
June 2006

Corresponding author address: Dr. Jia-Lin Lin
NOAA ESRL/CIRES Climate Diagnostics Center
325 Broadway, R/PSD1, Boulder, CO 80305-3328
Email: jialin.lin@noaa.gov

ABSTRACT

The Matsuno-Gill model has been widely used to study the tropical large-scale circulations and atmosphere-ocean interactions. However, a common critique of this model is that it requires a strong equivalent linear mechanical damping to get realistic wind response and it is unclear what could provide such a strong damping above the boundary layer. This study evaluates the sources and strength of equivalent linear mechanical damping in the Walker circulation by calculating the zonal momentum budget using 15 years (1979-1993) of daily global reanalysis data. Two different reanalyses (NCEP/NCAR and ERA-15) give qualitatively similar results for all major terms, including the budget residual, whose structure is consistent with its interpretation as eddy momentum flux convergence by convective momentum transport (CMT).

The Walker circulation is characterized by two distinct regions: a deep convection region over the Indo-Pacific warm pool, and a shallow convection region over the eastern Pacific cold tongue. These two regions are separated by a strong upper-troposphere ridge and a strong lower-troposphere trough in central Pacific. The resultant pressure gradient forces on both sides require strong (~ 5 days) damping to balance them because Coriolis force near the equator is too small to provide the balance. In the deep convection region, the damping is provided by CMT and advection together in both the upper and lower troposphere. In the shallow convection region, on the other hand, the damping is provided mainly by advection in the upper troposphere, and by CMT in the lower troposphere. In other words, the upper-level tropical easterly jet and the low-level trade wind are both braked by CMT. These results support the use of strong damping in the Matsuno-Gill type models. Implications for GCM's simulation of tropical mean climate are discussed.

1. Introduction

A widely used model for tropical large-scale circulations is the linear, dissipative model developed by Matsuno (1966) and revived by Gill (1980). The momentum equation of this model is simply linearized about a state at rest:

$$\partial \mathbf{V}/\partial t = -\nabla\varphi - f\,\mathbf{k} \times \mathbf{V} - \varepsilon\,\mathbf{V} \qquad (1)$$

where $\mathbf{V}$ is the wind, φ the geopotential, f the Coriolis parameter, and ε the linear damping coefficient; x and y are E-W and N-S distance. There are three acceleration terms: the pressure gradient force, the Coriolis force, and a linear damping. Amazingly, this simple model can reproduce quite well the basic features of the Walker circulation when using heating symmetric about the equator, and a qualitatively monsoon-like circulation when using linear sum of symmetric and asymmetric heatings (e.g. Gill 1980; Lau and Lim 1982; Silva Dias et al. 1983; DeMaria 1985; Zhang and Krishnamurti 1996). It has been combined with convective parameterization to simulate the atmospheric response to ENSO (e.g. Zebiak 1982; Seager 1991; Kleeman 1991), and has been frequently used to obtain the low-level atmospheric flow in simple coupled ocean-atmosphere models (e.g. Philander et al. 1984; Gill 1985; Anderson and McCreay 1985; Zebiak and Cane 1987; Schopf and Suarez 1988, Battisti 1988; Battisti and Hirst 1989, Wakata and Sarachik 1991).

Despite of the overall success of the Matsuno-Gill model, a common critique of this model is that it requires a rapid damping time scale (on the order of a few days, e.g. 1 day in Gill 1980) to get realistic wind responses, and it is unclear what could provide such a strong damping above the boundary layer, especially in the upper troposphere (see discussions by Battisti et al. 1999).

If we look at the large-scale momentum equation (cf. Eq. 2 below), there are two terms beside the pressure gradient force and Coriolis force: One is the advective tendency, and the other is the eddy momentum flux convergence (EMFC). These two terms are possible sources of the equivalent

linear damping. EMFC represents accelerations due to all subgrid-scale processes. Over open ocean, above the boundary layer, it is dominated by convective momentum transport (CMT; also called "cumulus friction" in some of the previous studies). Each of the terms in Eq. 2 except EMFC can be estimated from analyzed wind and pressure fields, and EMFC can be estimated from the residual of the budget. In this way, we can determine the contributions of the two possible damping terms to the momentum budget.

Several previous studies analyzed the momentum budget of tropical large-scale circulations both at the surface (e.g. Deser 1993, Wang and Li 1993, Chang et al. 2000) and in the free troposphere (Stevens 1979; Carr and Bretherton 2001; Tung and Yanai 2002a, b; Lin et al. 2005; and Dima et al. 2005). Deser (1993) evaluated the surface momentum budget over tropical Pacific Ocean using the Comprehensive Ocean-Atmosphere Data Set (COADS), derived the friction as a budget residual, and estimated the corresponding linear damping time scales. Stevens (1979) calculated the momentum budget for the GATE sounding array in tropical Atlantic Ocean, and found that CMT is as large as other acceleration terms in the synoptic-scale waves. Tung and Yanai (2003) studied the momentum budget for the TOGA COARE sounding array in western Pacific, and found that CMT contributes significantly to the Madden-Julian Oscillation (MJO) and two-day waves. Carr and Bretherton (2001) analyzed the momentum budget using TOGA COARE sounding array data as well as the NCEP and ECMWF reanalysis data during the TOGA COARE 4-month period (November 1992-Feburary 1993). The regions studied include not only the western Pacific, but also the central Pacific and eastern Pacific. They found that budget residual is significant at 850 mb in all three regions. Since the subcloud turbulent layer typically does not extend above 940 mb, this suggests an important role of CMT by shallow convection. Another important conclusion of the

Carr and Bretherton study is that uncertainties in budget results can be significantly reduced if they are averaged over a large domain and over a long time period.

Recently, Lin et al. (2005) examines the zonal momentum budget of the MJO over the equatorial western Pacific region using 15 years of daily NCEP and ECMWF reanalysis data. They found that the MJO is a highly viscous oscillation, with a 3–5-day equivalent linear damping time scale in the upper as well as lower troposphere. Upper-level damping is mainly in the form of large-scale advection terms, which are linear in MJO amplitude but involve horizontal and vertical background flow. Specifically, the leading terms are the advection of time-mean zonal shear by MJO vertical motion anomalies and advection of MJO wind anomalies by time-mean ascent. The strong upper-level damping necessitates upper-level geopotential height gradients to maintain the observed zonal wind anomalies over the time scales implied by the MJO's low frequency. The existence of the background flow thus tends to shift MJO temperature perturbations westward so that the warm anomaly ahead (east) of the convective center is shifted back into the convection. This shifting effect is fully realized only for anomalies with a period much longer than the 3–5-day damping time, and thus favors the amplification of the MJO more than other higher-frequency modes.

In this study, we extend the Carr and Bretherton (2001) and Lin et al. (2005) studies to the whole tropics. The purpose is to evaluate the sources and strength of mechanical damping in the Walker circulation. The issues we address are:

1. Is there a strong damping in the Walker circulation? i.e. Is the use of strong damping in the Matsuno-Gill type models supported by observation?
2. If there is a strong damping, what are the sources?

The datasets used in this study and the procedure for calculating zonal momentum budget are described in section 2. The quality of momentum budgets is evaluated in section 3 by looking at the

general features of budget residuals. Zonal momentum budget result of the Walker circulation is reported in section 4. Summary and discussions are given in section 5.

2. Data and method

The datasets used include 15 years (1979-1999) of daily reanalyses data from two different centers: NCEP (Kalnay et al. 1996) and ECMWF (the ERA-15 reanalysis, Gibson et al. 1999). The variables used include upper air wind, geopotential height, and vertical pressure velocity on pressure surfaces. The horizontal resolution is 2.5 degrees longitude by 2.5 degrees latitude. The zonal momentum budget is calculated for both reanalyses following Carr and Bretherton (2001), based on the large-scale momentum equation:

$$\partial \mathbf{V}/\partial t = -\nabla\varphi - f\,\mathbf{k}\times\mathbf{V} - (\mathbf{V}\bullet\nabla\,\mathbf{V} + \omega\partial\mathbf{V}/\partial p) + \mathbf{X} \qquad (2)$$

Here $\mathbf{X} = (X,Y)$ represents accelerations due to all subgrid-scale processes. Each budget term except $\mathbf{X}$ was calculated using daily average data at each 2.5 degree grid point. $\mathbf{X}$ is computed as the residual, meaning that all errors in the other terms are included in its observational estimate, requiring caution in interpretation. Derivatives were evaluated using 3-point central differencing. The results were then averaged to pentad mean along the equator (between 5N and 5S) with a zonal resolution of 10-degree longitude.

To study the convective activity, we also used 15 years (1979-1993) of pentad CMAP precipitation data (Xie and Arkin 1997) and 8 years (1986-1993) of 3-hourly ISCCP D1 cloud data (Rossow and Schiffer 1999). Both datasets were averaged to pentad mean along the equator (between 5N and 5S) with a zonal resolution of 10-degree longitude.

3. General features of the budget residuals

Before analyzing the scientific content of the budget results, the first question is how good the NCEP reanalysis and ECMWF reanalysis are in terms of the momentum budget. One way to evaluate this is to look at the budget residuals. Do they really represent the effect of CMT, or are they just some noises from data errors?

The existence of CMT requires two conditions: convection and vertical wind shear. Therefore if the budget residual does represent the effect of CMT, it should have good correlation with convection and wind shear both in space and in time. First we look at the spatial correlation. Fig. 1 shows the 15 year (1979-1993) DJF mean horizontal field of (a) CMAP precipitation, (b) NCEP 150 mb zonal wind, (c) NCEP 150 mb X, and (d) ECMWF 150 mb X. In the northern winter, the precipitation (Fig. 1a) centers slightly south of the equator. This region of the strongest convection also corresponds to the strongest vertical wind shear because of the upper level tropical easterly jet (Fig. 1b). The budget residual from NCEP reanalysis (Fig. 1c) also has it largest value over open ocean in this region, with a sign consistent with upward transport of westerly momentum. The ECMWF reanalysis shows similar feature but with a weaker magnitude (Fig. 1d).

Fig. 2 is same as Fig. 1 but for the northern summer. The center of the strongest convection moves to the north of the equator (Fig. 2a), together with the tropical easterly jet (Fig. 2b). The budget residual also moves northward following the convection and wind shear (Fig. 2c and Fig. 2d). Therefore, the budget residual correlates well in space with convection and vertical wind shear.

Next we look at the temporal correlation. Fig. 3 shows the scatter plot of budget residual versus the product of precipitation and 150mb-925mb vertical wind shear at one grid point (0N85E) for (a) NCEP reanalysis and (b) ECMWF reanalysis. The correlation is good for both the NCEP reanalysis

and the ECMWF reanalysis. This is also the case for other grid points we have checked. Therefore, the budget residuals correlate well in time with convection and vertical wind shear.

In short, the budget residuals correlate well with convection and vertical wind shear both spatially and temporally, suggesting that they do represent the effect of CMT, and the momentum budgets calculated from both reanalyses are useful. This is consistent with the results of Carr and Bretherton (2001).

4. Zonal momentum budget of the Walker circulation

Fig. 4 shows the longitude-height section of annual mean (a) ISCCP cloud fraction, (b) NCEP vertical motion, (c) NCEP zonal wind, and (d) NCEP geopotential height along the equator averaged between 5N and 5S. Zonal mean has been removed for geopotential height. Negative values are light-shaded, and continents are dark-shaded. As shown by Fig. 4a, the Walker circulation is characterized by two distinct regions: a deep convection region over the Indo-Pacific warm pool, and a shallow convection region over the eastern Pacific cold tongue. The large-scale vertical motion (Fig. 4b) is upward in the deep convection region, but downward in the shallow convection region. In the deep convection region, the zonal wind is characterized by strong easterly (tropical easterly jet) in the upper troposphere and weak westerly in the lower troposphere, while in the shallow convection region, it is characterized by strong westerly in the upper troposphere and strong easterly trade wind in the lower troposphere (Fig. 4c). Most important to this study, the deep convection region and shallow convection region are separated by a strong upper-troposphere ridge and a strong lower-troposphere trough in the central Pacific (Fig. 4d).

Fig. 5 is same as Fig. 4 but for the different components of the zonal momentum budget from NCEP reanalysis, including (a) pressure gradient force, (b) Coriolis force, (c) total advective

tendency, and (d) X. The upper-troposphere ridge in central Pacific (Fig. 4d) causes strong pressure gradient forces on both sides of it, as is shown in Fig. 5a. There is a westward pressure gradient force over the deep convection region, and an eastward pressure gradient force over the shallow convection region.

What balance these strong pressure gradient forces? Near the equator, the Coriolis force is small (Fig. 5b). In the deep convection region, NCEP reanalysis shows that the advection is also small (Fig. 5c), and the pressure gradient force is mainly balanced by the convective momentum flux convergence (Fig. 5d). In the shallow convection region, the strong pressure gradient force is balanced by advection (Fig. 5c), while the convective momentum transport is small (Fig. 5d).

The above results are from NCEP reanalysis. To give a quantitative comparison between the two reanalyses, following Carr and Bretherton (2001), we average the budget results over large domains, in this case, over the whole deep convection region and the whole shallow convection region. Fig. 6 shows the 15-year averaged vertical profiles for the deep convection region. The solid line is for NCEP reanalysis and the dashed line is for ECMWF reanalysis. To give an estimate of the error bars for the state variables and budget components, again, following Carr and Bretherton (2001), we over-plot in Fig. 6 the standard deviation of the differences between the two reanalyses for monthly mean data (the horizontal bars). We can see that the standard deviations are small, suggesting that the two reanalyses are quite consistent with each other. The deep convection region is characterized by climatological mean upward motion with the maximum around 300-400 mb (Fig. 6a), and the strong tropical easterly jet around 150 mb (Fig. 6b). There is a strong pressure gradient force in the upper troposphere (Fig. 6c), which is caused by the strong ridge in central Pacific (Fig. 4d). The strong pressure gradient force is balanced mainly by the advection below 175 mb (Fig. 6e), and by the convective momentum flux convergence above 175 mb (Fig. 6f).

How large, then, is the equivalent linear damping? Based on the definition of linear damping, we regress the monthly mean forces onto the monthly mean zonal wind to get an estimate of damping coefficient. Fig. 7 shows the vertical profiles of linear regression coefficients in unit of per day, i.e., 0.2 per day corresponds to a 5-day damping. The pressure gradient force (Fig. 7a) is equivalent to a 5 day forcing in the upper troposphere. That is to say, it requires a 5-day damping to balance it. This damping is provided and by the advection below 175 mb (Fig. 7c), and by the convective momentum flux convergence above 175 mb (Fig. 7e). The correlation coefficients (Figs. 7b, 7d, and 7f) are generally large whenever regression coefficients are large, suggesting that to the first-order approximation, it is appropriate to assume the corresponding mechanical damping terms to be linear.

The advective tendency (Fig. 7c) has three components: zonal, meridional, and vertical advection, which are plotted in Figs. 8a, b, and c, respectively. Actually, there are strong zonal (Fig. 8a) and meridional (Fig. 8b) advective tendencies above 200 mb, but they nearly cancel each other. The large total advective tendency below 200 mb (Fig. 7c) is mainly caused by the vertical component (Fig. 8c).

For the shallow convection region (Fig. 9), the two reanalyses both show upward motion in the lower levels and downward motion in the upper levels (Fig. 9a), consistent with the dominance of shallow cloud in this region (Fig. 4a). However, there is significant difference in the detailed shape of the vertical profile and the position of the peaks. This is not surprising because the vertical motion strongly depends on the convective parameterization (both the deep and shallow convection schemes) in the assimilation models. Fortunately, the significant difference in vertical motion between the two reanalyses does not cause much difference in the zonal momentum budget because the vertical advection is much smaller than other budget terms, as will be shown shortly in Fig. 11.

Unlike the vertical motion, the two reanalyses are quite consistent in zonal wind (Fig. 9b), and the zonal momentum budget terms (Fig. 9c-f). There is a strong pressure gradient force in both the upper and lower levels (Fig. 9c), which is caused by the central Pacific upper level ridge and lower level trough, respectively (Fig. 4d). In the upper level, the strong pressure gradient force is mainly balanced by advection (Fig. 9e), which agrees with the lack of deep convection in this region (Fig. 4a). In the lower level, the strong pressure gradient force is balanced by the convective momentum flux convergence (Fig. 9f), consistent with the abundance of shallow trade wind clouds in this region (Fig. 4a).

When scaled by the zonal wind, the pressure gradient force is equivalent to a 5-day forcing above 300 mb and a 5-day or larger forcing below 850 mb (Fig. 10a), which means that it requires such a strong damping to balance it. The damping in the upper troposphere is provided by the advective tendency (Fig. 10c), while that in the lower troposphere is provided by the convective momentum flux convergence (Fig. 10e). The correlation coefficients (Fig. 10b, 10d, 10f) are generally large whenever regression coefficients are large, suggesting that to the first-order approximation, it is appropriate to assume the corresponding mechanical damping terms to be linear.

The three components of the advective tendency (Fig. 10c) are plotted in Fig. 11. The strong advective tendency in the upper troposphere is contributed by both the zonal (Fig. 11a) and meridional (Fig. 11b) components. The vertical component is quite small in both reanalyses (Fig. 11c). Therefore, although the two reanalyses have substantial difference in vertical motion (Fig. 9a), it does not affect much the zonal momentum budget.

5. Summary and discussions

The Matsuno-Gill model has been widely used to study the tropical large-scale circulations and atmosphere-ocean interactions. However, a common critique of this model is that it requires a strong equivalent linear mechanical damping to get realistic wind response and it is unclear what could provide such a strong damping above the boundary layer. This study evaluates the sources and strength of equivalent linear mechanical damping in the Walker circulation by calculating the zonal momentum budget using 15 years (1979-1993) of daily global reanalysis data. Two different reanalyses (NCEP/NCAR and ERA-15) give qualitatively similar results for all major terms, including the budget residual, whose structure is consistent with its interpretation as eddy momentum flux convergence by convective momentum transport.

The zonal momentum budget of the Walker circulation is summarized schematically in Fig. 12. The Walker circulation is characterized by two distinct regions: a deep convection region over the Indo-Pacific warm pool, and a shallow convection region over the eastern Pacific cold tongue. These two regions are separated by a strong upper-troposphere ridge and a strong lower-troposphere trough in central Pacific. The resultant pressure gradient forces on both sides require strong (~ 5 days) damping to balance them because Coriolis force near the equator is too small to provide the balance. In the deep convection region, the damping is provided by CMT and advection together in both the upper and lower troposphere. In the shallow convection region, on the other hand, the damping is provided mainly by advection in the upper troposphere, and by CMT in the lower troposphere. In other words, the upper-level tropical easterly jet and the low-level trade wind are both braked by CMT. These results support the use of strong damping in the Matsuno-Gill type models.

The existence of strong convective momentum flux convergence at 150 mb in the deep convection region bears on the accuracy of the weak temperature gradient (WTG) scaling, which is being widely used in models of the tropical large-scale circulations (e.g. Sobel and Bretherton 2000, Sobel et al. 2001, Bretherton and Sobel 2002, 2003, Majda and Klein 2003). As discussed by Sobel et al. (2001), the WTG scaling is fundamentally a nearly inviscid scaling. Therefore the observed strong (~5 day) viscous damping in the deep convection region may need to be considered when evaluating the accuracy of WTG assumptions.

Our results have important implications for GCM's simulation of tropical mean climate. Because the convective momentum flux convergence is a dominant term of zonal momentum balance, and brakes both the upper-level tropical easterly jet and the lower-level trade winds, it needs to be considered in the GCMs. However, convective momentum transport has not been included in many GCMs, which makes the form of their zonal momentum balance questionable. GCM experiments have shown that the simulated tropical mean climate is very sensitive to the inclusion of CMT (e.g. Gregory et al. 1997; Inness and Gregory 1997; Wu et al. 2003). Gregory et al. (1997) found that including a CMT parameterization significantly weakens the upper level tropical easterly jet in the UKMO GCM, which is consistent with our observational results. Wu et al. (2003) found that including a CMT parameterization substantially improve the simulation of the seasonal migration of ITCZ in the NCAR GCM, which is caused by CMT-induced secondary meridional circulation. Another interesting result is that including a CMT parameterization significantly alleviated the double-ITCZ problem (i.e. insufficient precipitation on the equator in the warm pool region but excessive precipitation off the equator) in the GFDL GCM (Isaac Held 2004, personal communication). This may be understood based on the model of tropical mean climate by Wang and Li (1993), which is a Matsuno-Gill type model with a frictional boundary

layer. They found that when the frictional layer is thin, the climatological mean precipitation tends to show a double-ITCZ pattern with maximum precipitation off the equator and little precipitation on the equator, but when the frictional layer is thick, the double-ITCZ pattern disappears and the maximum precipitation concentrates on the equator (see Wang and Li 1993, their Figs. 10a, b). This may be because a thicker frictional layer favors precipitation over the region with the highest low-level moisture (which in turn is the region with the warmest SST right on the equator) through the frictional Wave-CISK mechanism. As shown in Fig. 7e and Fig. 10e, the shallow convective momentum transport causes strong mechanical damping above the boundary layer up to 850 mb, which makes the frictional layer much thicker than the boundary layer (usually with top below 940 mb) and thus may help to alleviate the double-ITCZ problem. Unfortunately, convective momentum transport has not been included in many GCMs. Several schemes have been developed (e.g, Zhang and Cho 1991a,b, Tiedke 1993, Wu and Yanai 1994, Kershaw and Gregory 1997, and Zhu and Bretherton 2004), and the results of current study provide a baseline for evaluating the parameterization of these schemes.

Acknowledgments

This study benefits from the discussions with Hua-Lu Pan, Klaus Weickmann, George Kiladis, Clara Deser, Adam Sobel, and Xiaoqing Wu. This work was supported by U.S. CLIVAR CMEP Project, NOAA OGP CLIVAR-Pacific Program, and NASA MAP Program.

REFERENCES

Anderson, D., and J. P. McCreary, 1985: Slowly propagating disturbances in a coupled ocean-atmosphere model. J. Atmos. Sci., **42**, 615-629.

Battisti, D. S., 1988: Dynamics and thermodynamics of a warming event in a coupled tropical atmosphere-ocean model. J. Atmos. Sci., **45**, 2889-2919.

Battisti, D. S., and A. C. Hirst, 1989: Interannual variability in a tropical atmosphere-ocean model: Influence of the basic state, ocean geometry and nonlinearity. J. Atmos. Sci., **46**, 1687-1712.

Battisti, D. S., Sarachik, E. S., Hirst, A. C.. 1999: A Consistent Model for the Large-Scale Steady Surface AtmosphericCirculation in the Tropics. J. Climate, **12**, 2956-2964.

Bretherton, C. S., and A. H. Sobel, 2002: A simple model of a convectively coupled Walker circulation using the weak temperature gradient approximation. *J. Climate.,* **15**, 2907–2920.

Bretherton, C., and A. Sobel, 2003: The Gill model and the weak temperature gradient approximation. *J. Atmos. Sci.,* **60**, 451–460.

Carr, M. T., Bretherton, C. S. 2001: Convective Momentum Transport over the Tropical Pacific: Budget Estimates. J. Atmos. Sci., **58**, 1673-1693.

Chiang, J.C.H., and S. E. Zebiak. 2000: Surface Wind over Tropical Oceans: Diagnosis of the Momentum Balance, and Modeling the Linear Friction Coefficient. Journal of Climate: Vol. 13, No. 10, pp. 1733–1747.

Davey, M. K., and A. Gill, 1987: Experiments on tropical circulation with a simple moist model. Quart. J. Roy. Meteor. Soc., **113**, 1237-1269.

Deser. C., 1993: Diagnosis of the Surface Momentum Balance over the Tropical Pacific Ocean. Journal of Climate: Vol. 6, No. 1, pp. 64–74.

Dima, I. M., J. M. Wallace and I. Kraucunas. 2005: Tropical Zonal Momentum Balance in the NCEP Reanalyses. Journal of the Atmospheric Sciences: Vol. 62, No. 7, pp. 2499–2513.

Gill, A. E., 1980: Some simple solutions for heat induced tropical circulation. Quart. J. Roy. Meteor. Soc., **106**, 447-462.

Gill, A. E., 1985: Elements of coupled ocean-atmosphere models for the tropics. Coupled Ocean-Atmosphere Models, J. Nihoul, Ed., Elsevier Oceanography Series, Vol. 40, Elsevier, 303-327.

Gregory, D., R. Kershaw, and P. M. Inness, 1997: Parametrization of momentum transport by convection. II: Tests in single-column and general circulation models. *Quart. J. Roy. Meteor. Soc.,* **123,** 1153–1183.

Hirst, A. C., 1986: Unstable and damped equatorial modes in simple coupled models. J. Atmos. Sci., 43, 606-630.

Inness, P. M., and D. Gregory, 1997: Aspects of the intraseasonal oscillation simulated by the Hadley Centre atmospheric model. Clim Dyn 13:441-458

Kleeman, R., 1991: A simple model of the atmospheric response to ENSO sea surface temperature anomalies. J. Atmos. Sci., 48, 3-18.

Kershaw, R., and D. Gregory, 1997: Parametrization of momentum transports by convection. I: Theory and cloud modeling results. *Quart. J. Roy. Meteor. Soc.,* **123**, 1133–1151.

Lau, K-M, and H. Lim, 1982: Thermally Driven Motions in an Equatorial β-Plane: Hadley and Walker Circulations During the Winter Monsoon. *Monthly Weather Review*: Vol. 110, No. 5, pp. 336–353.

Lin, J. L., M. H. Zhang, and B. E. Mapes, 2005: Zonal momentum budget of the Madden-Julian Oscillation: The sources and strength of equivalent linear damping. *J. Atmos. Sci.*, **62**, 2172-2188.

Majda, A. J., and R. Klein, 2003: Systematic multiscale models for the Tropics. *J. Atmos. Sci.,* **60**, 393–408.

Matsuno, T., 1966: Quasi-geostrophic motions in the equatorial area. J. Meteor. Soc. Japan, 44, 25-43.

Neelin, J. D., 1988: A simple model for the surface stress and low level flow in the tropical atmosphere driven by prescribed heating. Quart. J. Roy. Meteor. Soc., 114, 747-770.

Philander, S., T. Yamagata, and R. Pacanowski, 1984: Unstable air-sea interactions in the Tropics. J. Atmos. Sci., **41**, 604-613.

Schopf, P. S., and M. J. Suarez, 1988: Vacillations in a coupled ocean-atmosphere model. J. Atmos. Sci., **45**, 549-566.

Seager, R., 1991: A simple model of the climatology and variability of the low-level wind field in the Tropics. J. Climate, **4**, 164-179.

Sobel, A. H., and C. S. Bretherton, 2000: Modeling tropical precipitation in a single column. *J. Climate.,* **13**, 4378–4392.

Sobel, A. H., J. Nilsson, and L. M. Polvani, 2001: The weak temperature gradient approximation and balanced tropical moisture waves. *J. Atmos. Sci.,* **58**, 3650–3665.

Sui, C.-H., and M. Yanai, 1986: Cumulus ensemble effects on the large-scale vorticity and momentum fields of GATE. Part I: Observational evidence. J. Atmos. Sci., 43, 1618-1642.

Tiedtke, M., 1993: Representation of clouds in large-scale models. *Mon. Wea. Rev.,* **121**, 3040–3061.

Tung, W. W., Yanai, M., 2002a: Convective Momentum Transport Observed during the TOGA COARE IOP. Part I: General Features. J. Atmos. Sci., **59**, 1857-1871.

Tung, W. W., Yanai, M., 2002b: Convective Momentum Transport Observed during the TOGA COARE IOP. Part II: Case Studies. J. Atmos. Sci., **59**, 2535-2549.

Wang, B., and T. Li. 1993: A Simple Tropical Atmosphere Model of Relevance to Short-Term Climate Variations. *J. Atmos. Sci.*, **50**, 260–284.

Wakata, Y., and E. S. Sarachik, 1991: Unstable coupled atmosphere-ocean basin modes in the presence of a spatially varying basic state. J. Atmos. Sci., **48**, 2060-2077.

Webster, Peter J., Chang, Hai-Ru. 1988: Equatorial Energy Accumulation and Emanation Regions: Impacts of a Zonally Varying Basic State. *J. Atmos. Sci.,* **45**, 803–829.

Wu, X., and M. Yanai, 1994: Effects of vertical wind shear on the cumulus transport of momentum: Observations and parameterization. *J. Atmos. Sci.,* **51**, 1640–1660.

Wu, X., X.-Z. Liang, and G. J. Zhang, 2003: Seasonal migration of ITCZ precipitation across the equator: Why can't GCMs simulate it? Geophys. Res. Lett., 30, 1824, doi:10.1029/2003GL017198.

Zebiak, S. E., and M. Cane, 1987: A model El Niño/Southern Oscillation. Mon. Wea. Rev., **115**, 2262-2278.

Zhang, G. J., and H. R. Cho, 1991a: Parameterization of the vertical transport of momentum by cumulus clouds. Part I: Theory. *J. Atmos. Sci.,* **48**, 1483–1492.

Zhang, G. J., and H. R. Cho, 1991b: Parameterization of the vertical transport of momentum by cumulus clouds. Part II: Application. *J. Atmos. Sci.,* **48**, 2448–2457.

Zhang, Z., Krishnamurti, T.N.. 1996: A Generalization of Gill's Heat-Induced Tropical Circulation. *J. Atmos. Sci.*, **53**, 1045–1056.

Zhu, P., and C. S. Bretherton, 2004: A Simulation Study of Shallow Moist Convection and Its Impact on the Atmospheric Boundary Layer. Mon. Wea. Rev., 132, 2391-2409.

FIGURE CAPTIONS

Fig. 1 15 year DJF mean horizontal field of (a) CMAP precipitation (mm/day), (b) NCEP 150 mb zonal wind (m/s), (c) NCEP 150 mb X (m/s/day), and (d) ECMWF 150 mb X (m/s/day).

Fig. 2 As in Fig. 1 except for JJA.

Fig. 3 Scatter diagrams of monthly mean 150 mb X versus the product of CMAP precipitation and zonal wind shear between 150 mb and 925 mb for (a) NCEP data, and (b) ECMWF data.

Fig. 4 Annual mean (a) cloud fraction for 8 years (1986-1993) of ISCCP D1 data, and (b) ω (mb/day), (c) u (m/s), and (d) Z (m, from which zonal mean is removed) for 15 years (1979-1993) of NCEP reanalysis data along the equator averaged between 5N-5S. Negative values are light-shaded. Continents are dark-shaded.

Fig. 5 As in Fig. 4 except for (a) pressure gradient force, (b) Coriolis force, (c) total advective tendency, and (d) residual. Unit is m/s/day.

Fig. 6 Vertical profile of annual mean (a) ω, (b) u, (c) pressure gradient force, (d) Coriolis force, (e) advective tendency, and (f) budget residual for 15 years (1979-1993) of NCEP (solid line) and ECMWF (dashed line) reanalyses data averaged over the deep convection region (80E-160E and 5N-5S).

Fig. 7 Vertical profile of linear regression coefficient of the monthly mean (a) pressure gradient force, (c) advective tendency, and (e) budget residual, with respect to the zonal wind at the same level for 15 years (1979-1993) of NCEP (solid line) and ECMWF (dashed line) reanalyses data averaged over the deep convection region (80E-160E and 5N-5S). The corresponding correlation coefficients are shown in (b), (d), and (f), respectively.

Fig. 8 As in Fig. 7 except for (a) zonal, (b) meridional, and (c) vertical component of advective tendency.

Fig. 9 As in Fig. 6 except for the shallow convection region (180E-240E, 5N-5S).

Fig. 10 As in Fig. 7 except for the shallow convection region (180E-240E, 5N-5S).

Fig. 11 As in Fig. 8 except for the shallow convection region (180E-240E, 5N-5S).

Fig. 12 Schematic depiction of the zonal momentum budget of the Walker circulation. ``H'' and ``L'' represent the high and low geopotential heights, respectively. Thin arrows represent the winds. Thick arrows represent the components of zonal momentum budget.

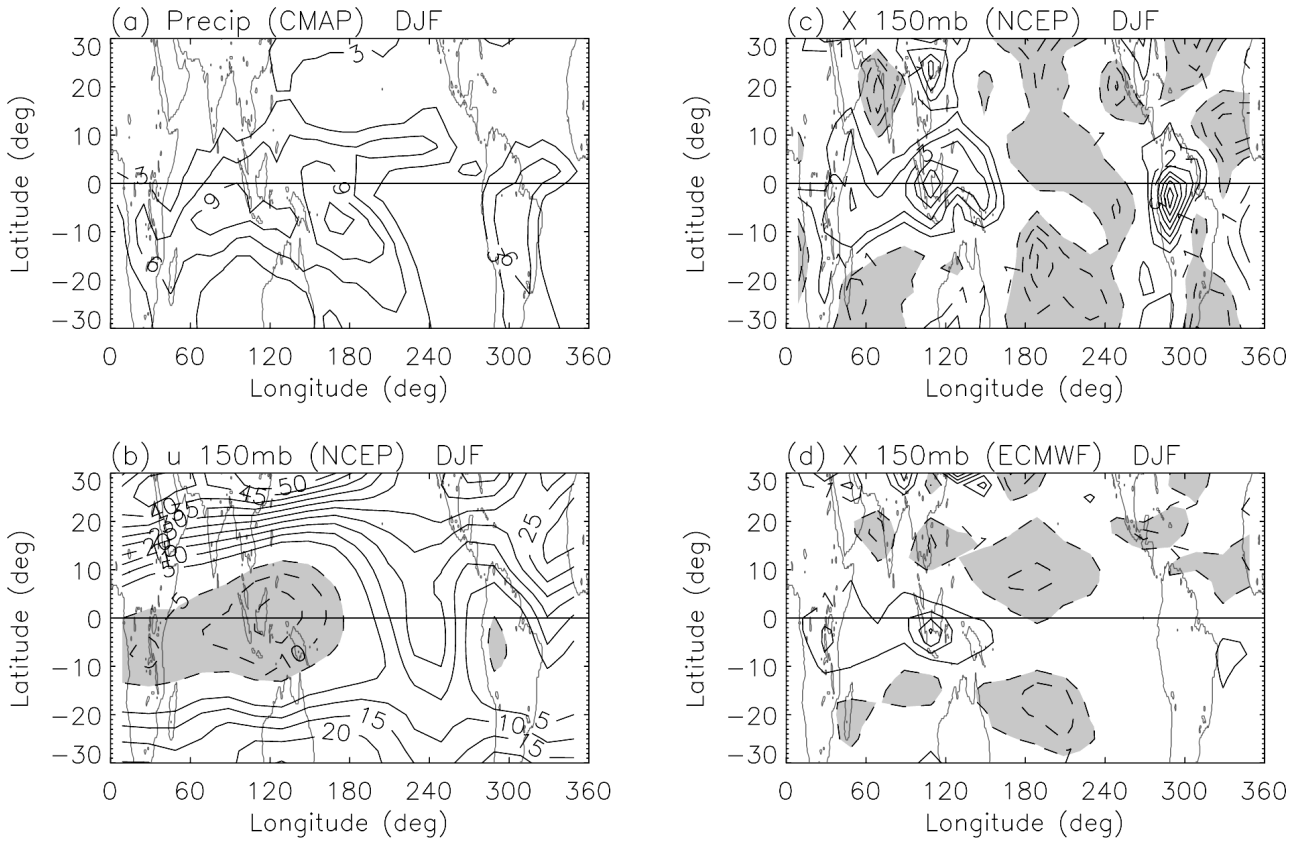

Fig. 1 15 year DJF mean horizontal field of (a) CMAP precipitation (mm/day), (b) NCEP 150 mb zonal wind (m/s), (c) NCEP 150 mb X (m/s/day), and (d) ECMWF 150 mb X (m/s/day).

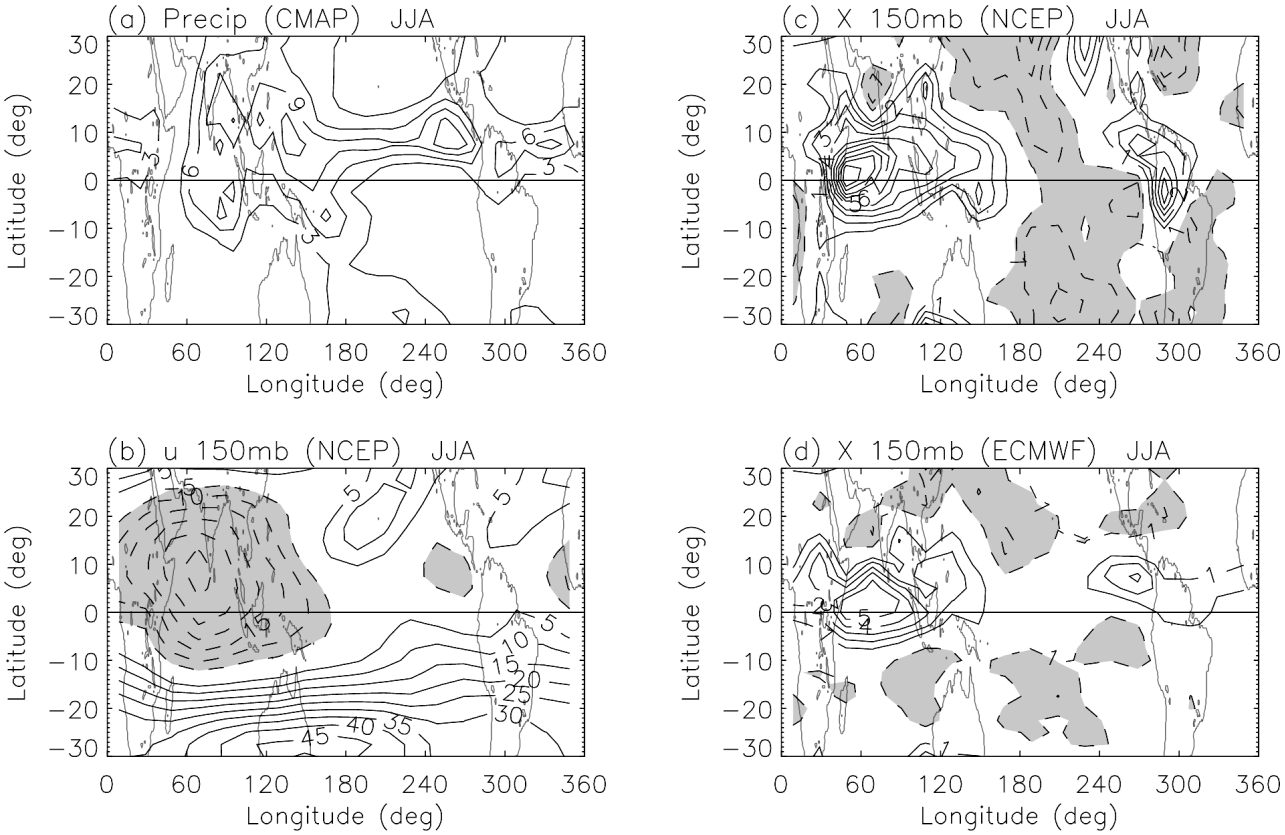

Fig. 2 As in Fig. 1 except for JJA.

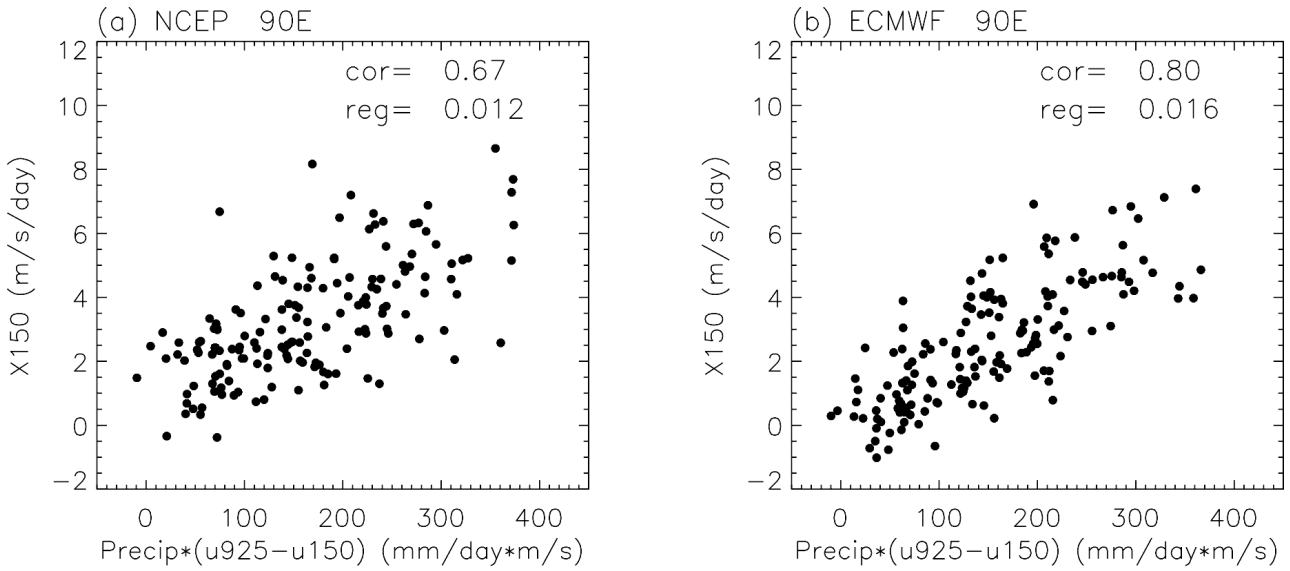

Fig. 3 Scatter diagrams of monthly mean 150 mb X versus the product of CMAP precipitation and zonal wind shear between 150 mb and 925 mb for (a) NCEP data, and (b) ECMWF data.

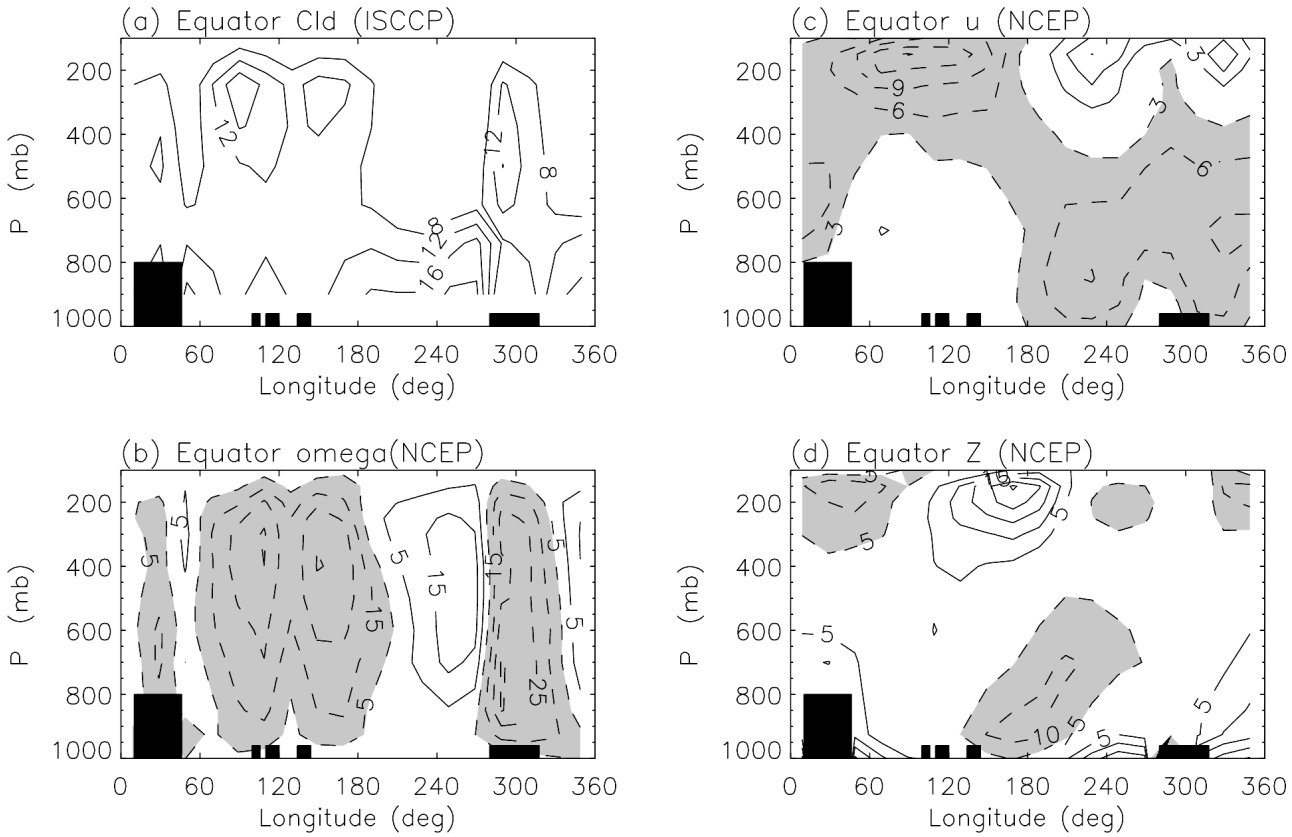

Fig. 4 Annual mean (a) cloud fraction for 8 years (1986-1993) of ISCCP D1 data, and (b) ω (mb/day), (c) u (m/s), and (d) Z (m, from which zonal mean is removed) for 15 years (1979-1993) of NCEP reanalysis data along the equator averaged between 5N-5S. Negative values are light-shaded. Continents are dark-shaded.

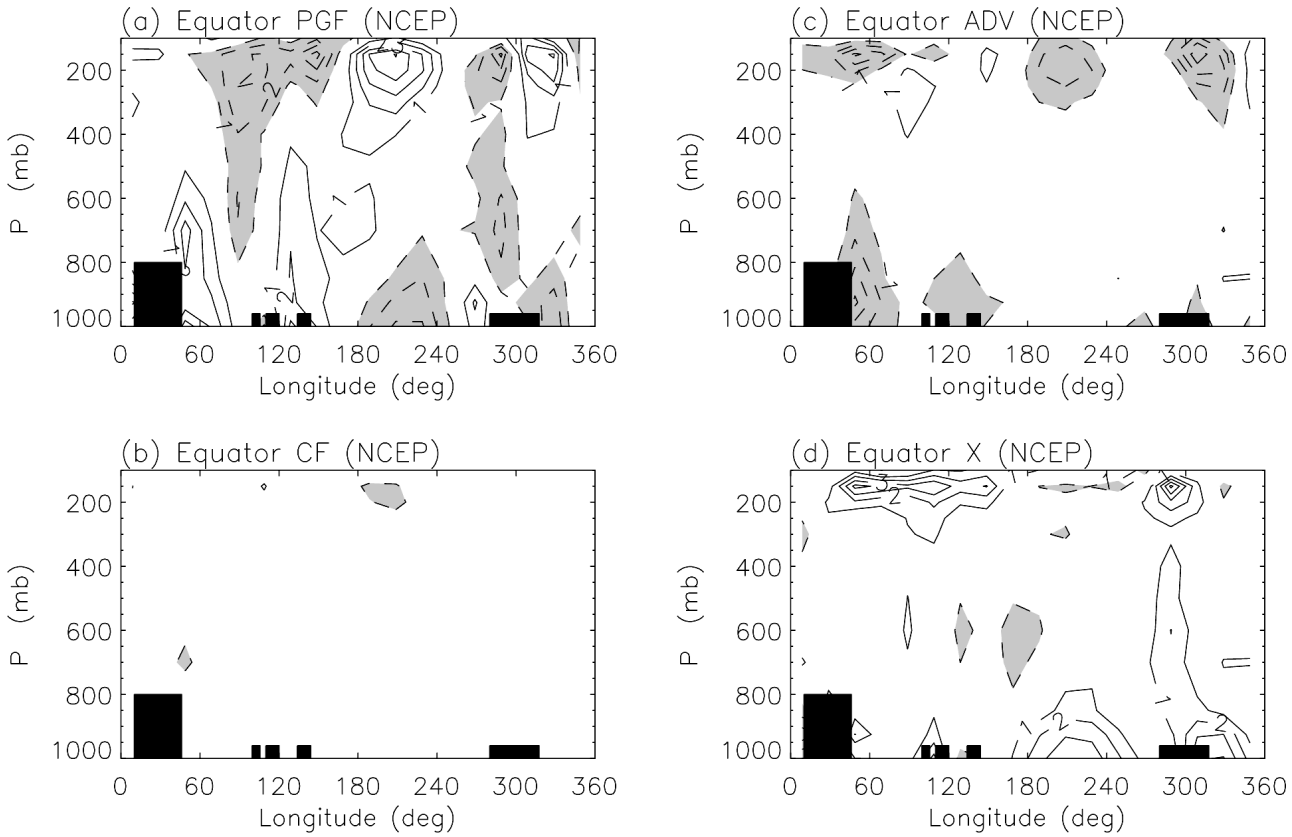

Fig. 5 As in Fig. 4 except for (a) pressure gradient force, (b) Coriolis force, (c) total advective tendency, and (d) residual. Unit is m/s/day.

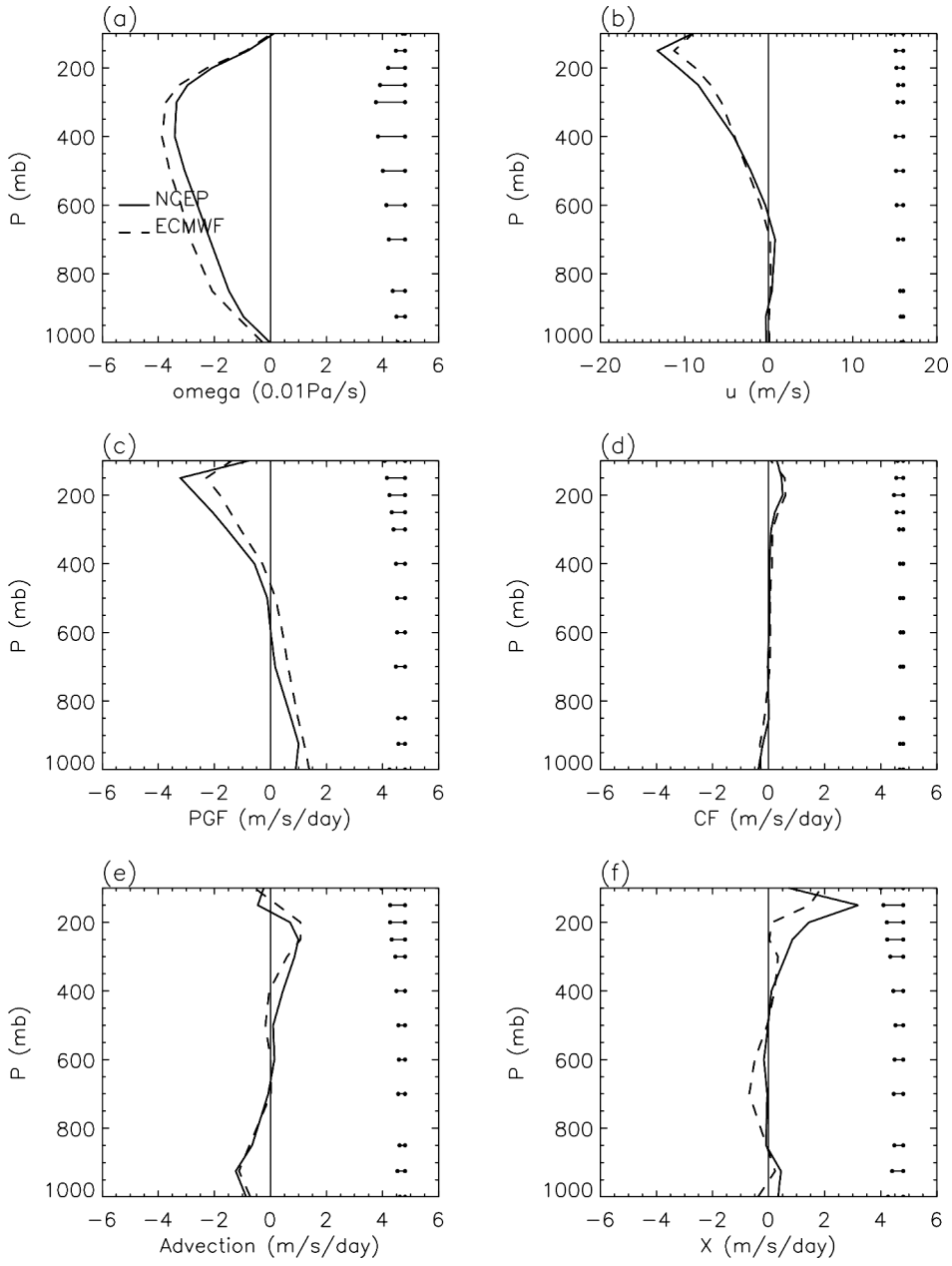

Fig. 6 Vertical profile of annual mean (a) ω, (b) u, (c) pressure gradient force, (d) Coriolis force, (e) advective tendency, and (f) budget residual for 15 years (1979-1993) of NCEP (solid line) and ECMWF (dashed line) reanalyses data averaged over the deep convection region (80E-160E and 5N-5S).

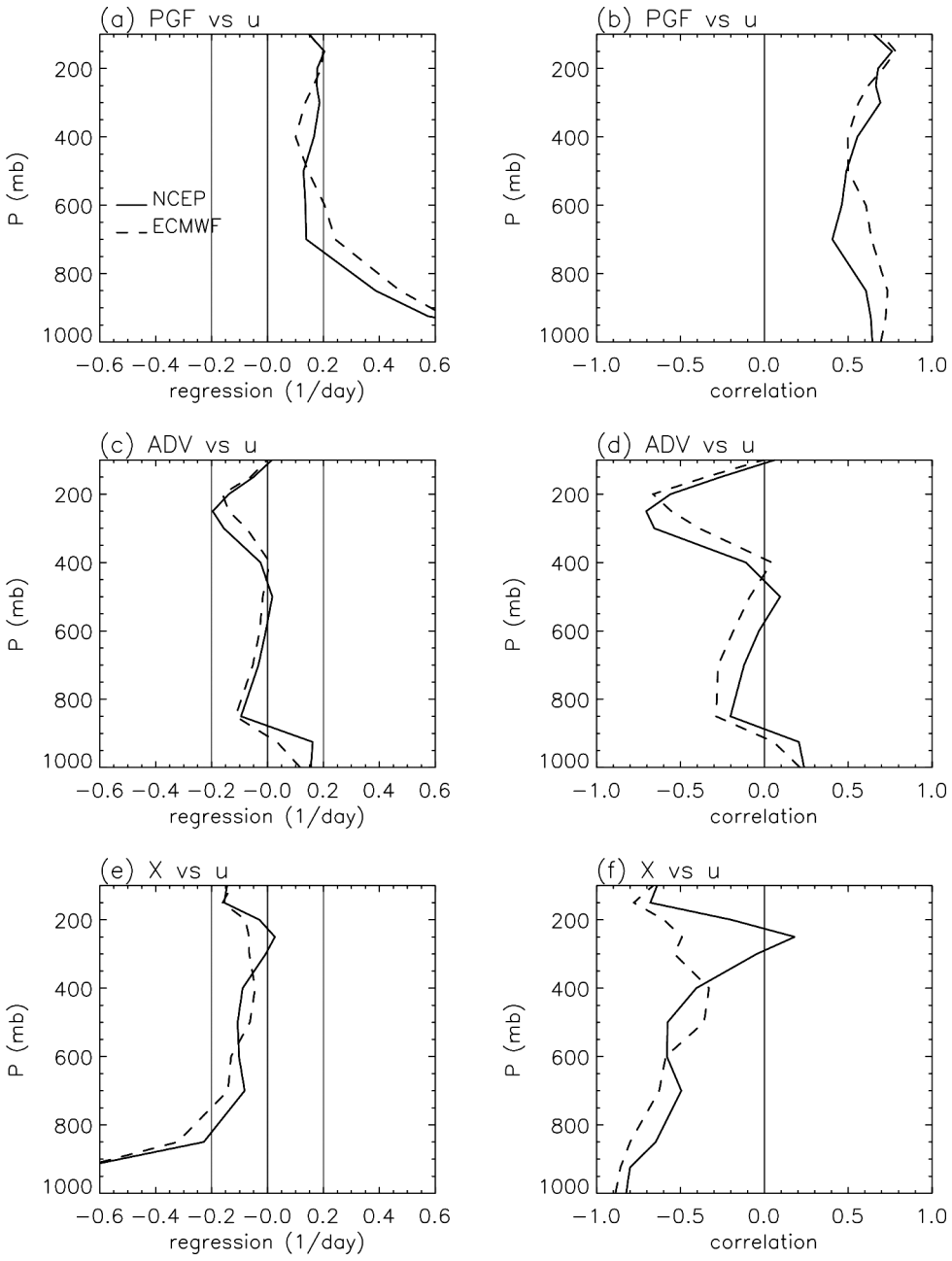

Fig. 7 Vertical profile of linear regression coefficient of the monthly mean (a) pressure gradient force, (c) advective tendency, and (e) budget residual, with respect to the zonal wind at the same level for 15 years (1979-1993) of NCEP (solid line) and ECMWF (dashed line) reanalyses data averaged over the deep convection region (80E-160E and 5N-5S). The corresponding correlation coefficients are shown in (b), (d), and (f), respectively.

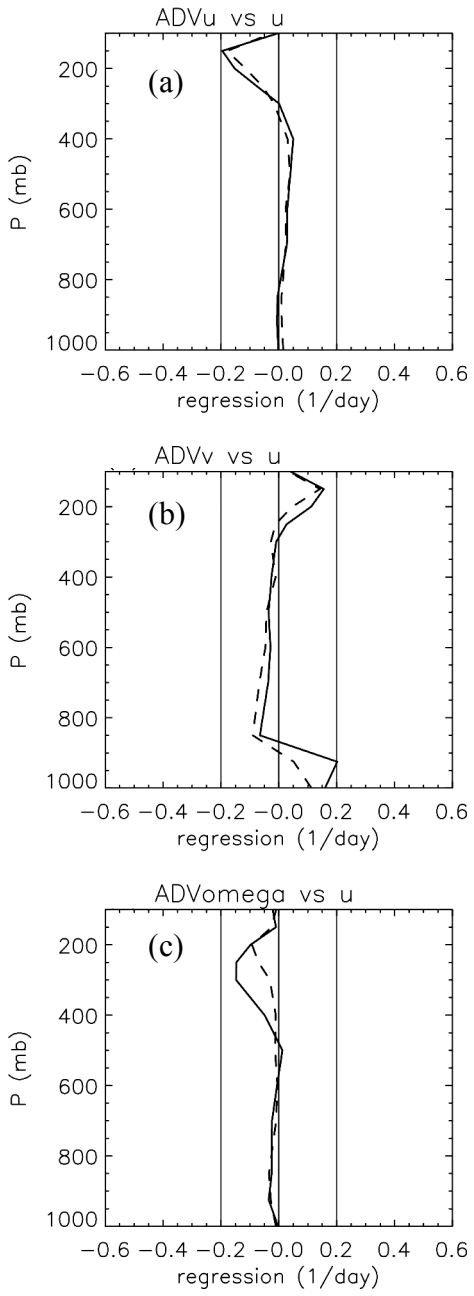

Fig. 8 As in Fig. 7 except for (a) zonal, (b) meridional, and (c) vertical component of advective tendency.

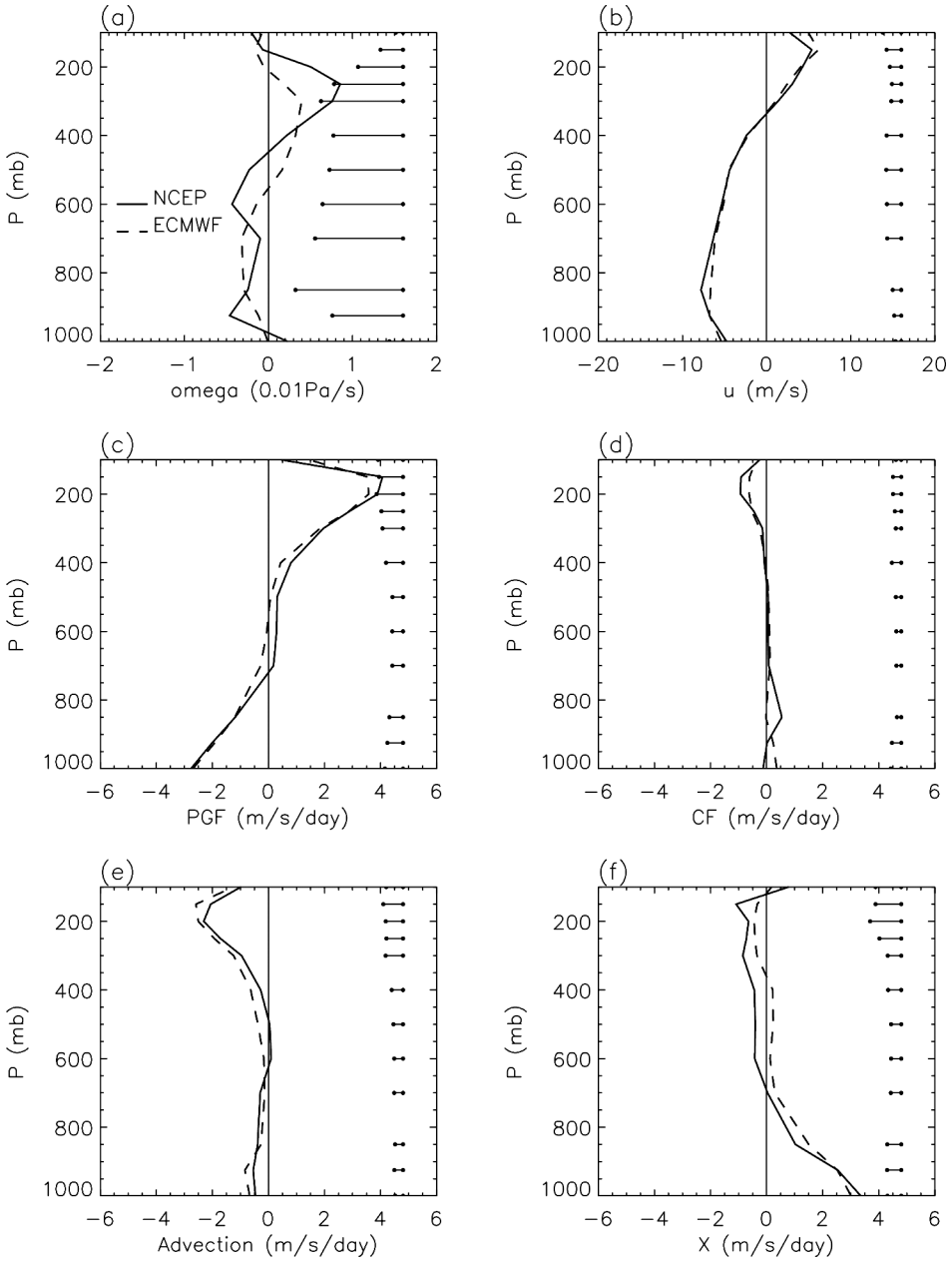

Fig. 9 As in Fig. 6 except for the shallow convection region (180E-240E, 5N-5S).

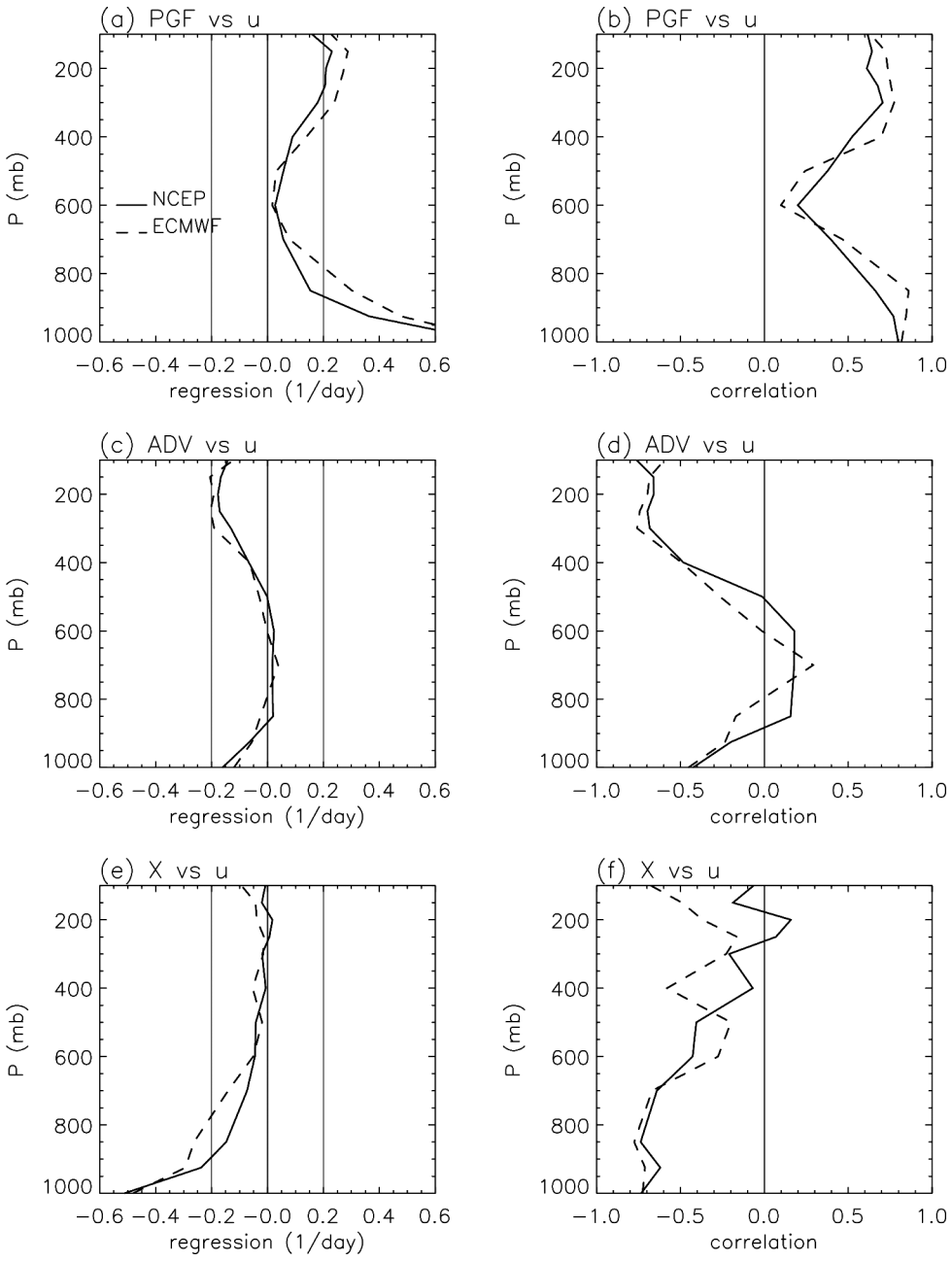

Fig. 10 As in Fig. 7 except for the shallow convection region (180E-240E, 5N-5S).

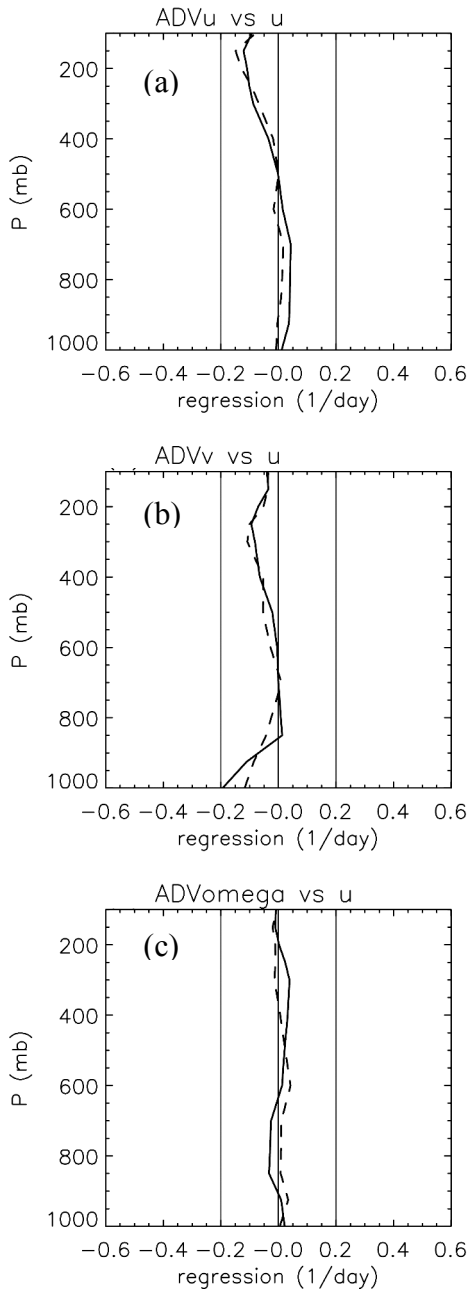

Fig. 11 As in Fig. 8 except for the shallow convection region (180E-240E, 5N-5S).

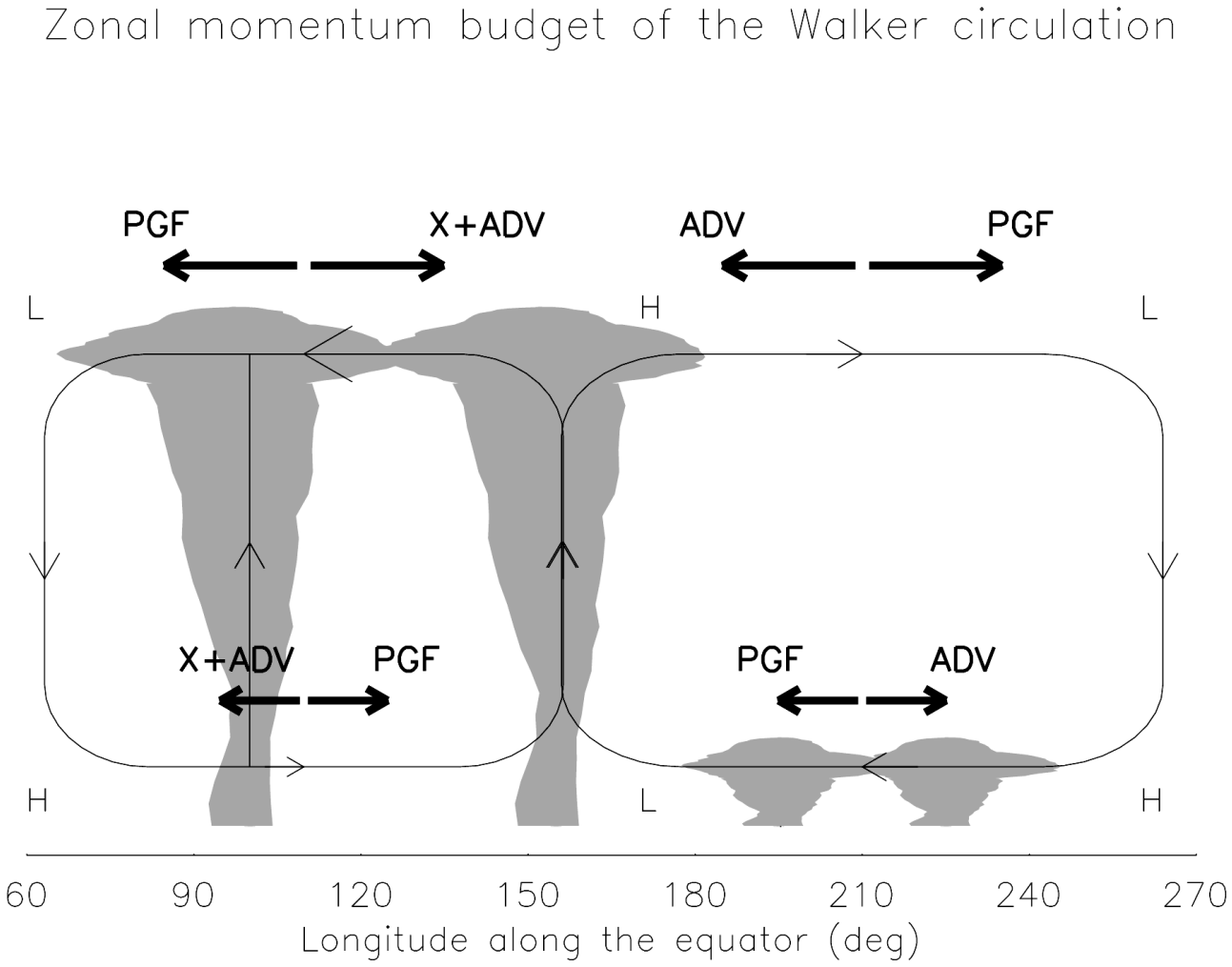

Fig. 12 Schematic depiction of the zonal momentum budget of the Walker circulation. ``H'' and ``L'' represent the high and low geopotential heights, respectively. Thin arrows represent the winds. Thick arrows represent the components of zonal momentum budget.